

Application of Supramolecular Bidentate Hybrid Ligands in Asymmetric Hydroformylation

Rosalba Bellini and Joost N. H. Reek*^[a]

Abstract: In this study we report a novel class of supramolecular bidentate hybrid ligands in which the two inequivalent phosphorus units and pyridine moieties are covalently attached to a chiral scaffold and the supramolecular interactions are used as a second handle to control the coordination sphere around the transition-metal centre. The coordination chemistry of these ligands was investigated under hydroformylation conditions by high-

pressure NMR and IR spectroscopy, revealing the formation of a single active species in which the phosphane ligand is in the axial position and the phosphoramidite adopts the equatorial position. These ligands were applied in

Keywords: hydroformylation • ligand design • IR spectroscopy • NMR spectroscopy • supramolecular chemistry

the asymmetric Rh-catalysed hydroformylation of styrene and *para*-substituted analogues. In these hydroformylation reactions, modification of the electronic and steric properties of the zinc(II)-templates appear to have a significant influence on the activity and selectivity of the catalysis. In particular, zinc(II)-templates bearing more electron-withdrawing substituents led to an increase in enantioselectivity.

Introduction

Asymmetric hydroformylation (AHF) is a powerful and efficient homogeneous catalytic process that transforms alkenes and syngas (H₂/CO) into chiral aldehydes in a single step with 100% atom efficiency.^[1] The chiral aldehydes are highly valuable products that can be used as important precursors for a variety of pharmaceutical and fine chemical intermediates.^[2] Although the reaction is extremely attractive for both industry and academia, AHF has not been frequently used in organic synthesis. One important reason lies in the difficulty of controlling both the regio- and enantioselectivity at moderately high temperature while still obtaining reasonable reaction rates. This is usually a highly challenging task because higher temperatures are required to obtain sufficient reaction rates, but this often is associated with a decrease in regio- and enantioselectivity. The most efficient way to control these selectivities, besides altering reaction parameters such as pressure and temperature, is by employing chiral ligands that are able to steer the reaction towards the desired product. Therefore, in the field of Rh-catalysed AHF, significant efforts have been directed towards the design and development of new chiral ligands. Over the past three decades, although a large variety of chiral ligands have

been examined, excellent results were reported only for a small number of ligands. Most of these ligands are bidentate and rely on relatively π -acidic phosphorus atoms such as phosphite, phosphoramidites, phospholanes and diazaphospholanes to achieve good reaction rates. Bidentate phosphite ligands such as (2*R*,4*R*)-Chiraphite^[3] exhibit good enantioselectivity in the reaction of styrene. (*S,S*)-Kelliphite^[4] is more efficient in the stereocontrol of HF of allyl cyanide and vinyl acetate. Wills and co-workers reported the first phospholane-type ligand, (*S,S*)-Esphos,^[5] which was effective for the AHF of vinyl acetate. Landis, Klosin and co-workers introduced the diazaphospholane ligands, which displayed effective control over regio- and enantioselectivities in the AHF of styrene, vinyl acetate and allyl cyanide (Figure 1).^[6] The most successful class of ligands for Rh-catalysed AHF are hybrid ligands containing a phosphane and either a phosphite or a phosphoramidite. In this field a major breakthrough was achieved with (*R,S*)-Binaphos, developed by Takaya, Nozaki and co-workers in 1993 (Figure 2, **I**).^[7] This catalyst turned out to be extremely versatile, giving *ee* values up to 95% for a wide range of substrates. More recently, Zhang, Yang and co-workers reported a phosphoramidite analogue of Binaphos, (*R,S*)-YanPhos, which significantly improved the enantioselectivity over (*R,S*)-Binaphos in AHF of styrenes and vinyl acetate (Figure 2, **II**).^[8] Other successful examples of hybrid bidentate ligands are depicted in Figure 2 and were developed by the groups of van Leeuwen (**III**),^[9] Claver (**IV**),^[10] Pizzano and Peruzzini (**V**),^[11] Clarke (**VI**),^[12] Schmalz (**VII**),^[13] and Reek (**VIII** and **IX**).^[14]

An alternative way to generate bidentate hybrid ligands involves the self-assembly of monodentate units to bidentate ligands employing noncovalent interactions such as hydro-

[a] R. Bellini, Prof. Dr. J. N. H. Reek
Van't Hoff Institute for Molecular Science
University of Amsterdam
Science Park 904, Amsterdam 1098 XH (The Netherlands)
Fax: (+31) 205255604
E-mail: j.n.h.reek@uva.nl

Supporting information for this article is available on the WWW under <http://dx.doi.org/10.1002/chem.201202044>.

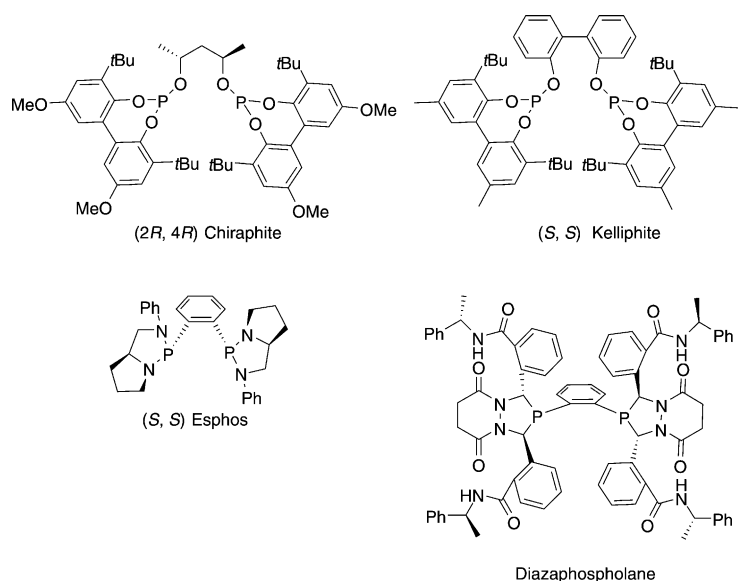


Figure 1. Representative examples of chiral bidentate ligands successfully used in AHF of alkenes.

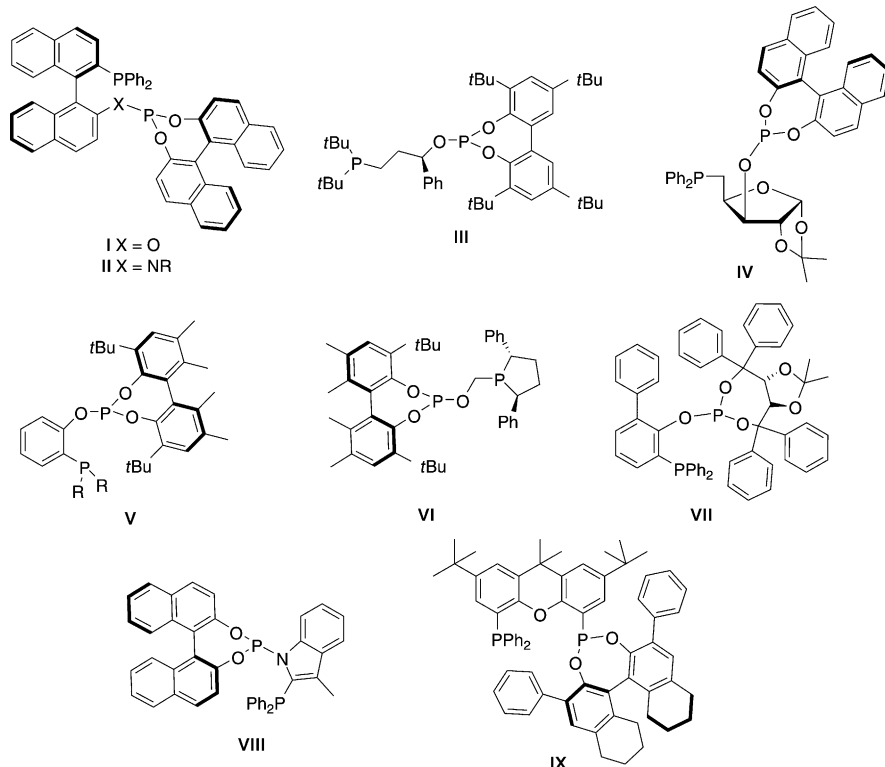


Figure 2. Representative examples of chiral bidentate hybrid ligands for AHF of alkenes.

gen bonds, ionic interactions or dynamic metal-ligand coordination.^[15] Our group has reported examples of supramolecular bidentate ligands based on coordinative bonding between phosphane or phosphite ligands functionalised with pyridine moieties and zinc(II)-templates. Successful examples of these assemblies in AHF are reported in Figure 3. Formation of chelating supramolecular hybrid bidentate li-

gands was obtained by self-assembly of two different monodentate building blocks on a rigid bis-zinc(II)-salphen building block (Figure 3, **A**).^[16] In the AHF of styrene this assembly gave *ee* values up to 72%. An alternative approach involves combining different monodentate ligand building blocks equipped with complementary binding sites to form hybrid bidentate ligands. Through the preparation of 40 building blocks, a ligand library of 400 ligands was created (Supraphos). The application of a part of this library of chelating hybrid ligands in AHF of styrene gave *ee* values up to 76% (Figure 3, **B**).^[17]

Further development of this concept led us to search for alternative strategies to form supramolecular bidentate hybrid ligands. In this contribution we introduce a new class of supramolecular bidentate ligands in which the two inequivalent phosphorus units and the pyridine moieties are covalently attached to a chiral scaffold and the supramolecular interactions are used as an additional handle to increase the steric bulk and eventually encapsulate the transition-metal centre (Figure 4). The supramolecular assembly is formed in situ by selective interactions between

the nitrogen donor atoms and the zinc(II) template, which will result in the encapsulation of the transition-metal centre that is used for catalysis. In addition, we demonstrate that we can influence the ligand properties by using electronically and sterically different zinc(II) templates. In asymmetric hydroformylation of styrene and *p*-styrene derivatives, the different supramolecular ligands change dramatically key reaction features such as activity and selectivity, which illustrates the high versatility of these new systems.

Ligand synthesis: The novel bidentate phosphane-phosphoramidite ligands (*S*)-**1a–c** were prepared according to the procedure depicted in Scheme 1. The synthetic procedure started with the conversion of *N*-methylaniline (**1**) into the corresponding lithium carbamate compound, followed by *o*-lithiation with *t*BuLi and treatment

with Ph₂PCl and subsequent hydrolysis to give compound **2**.^[18] Phosphane **2** was transformed into **3** by reaction with PCl₃ at low temperature and under basic conditions. Quantitative yields were achieved and the phosphorodichloride compound was used in the next step without any further purification. Compounds (*S*)-**6a–c** were prepared starting from the reduction of the commercially available (*S*)-binol in the

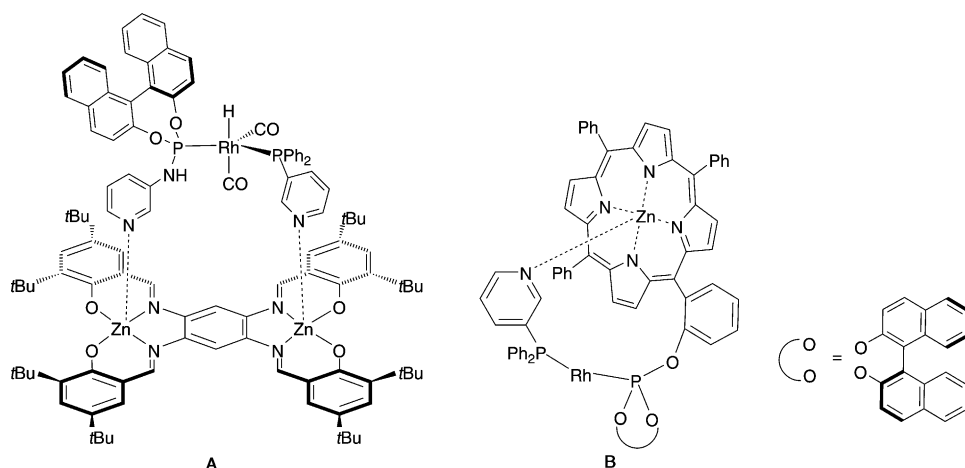


Figure 3. Formation of hybrid bidentate ligands by self-assembly of complementary units.

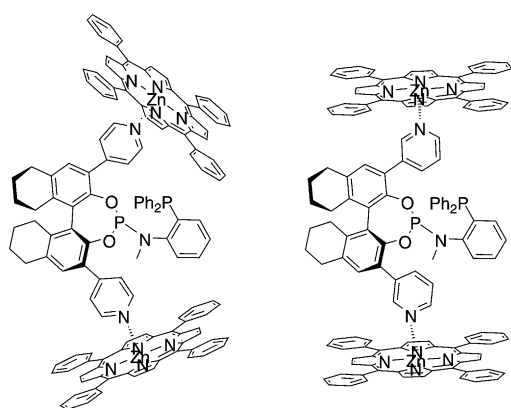
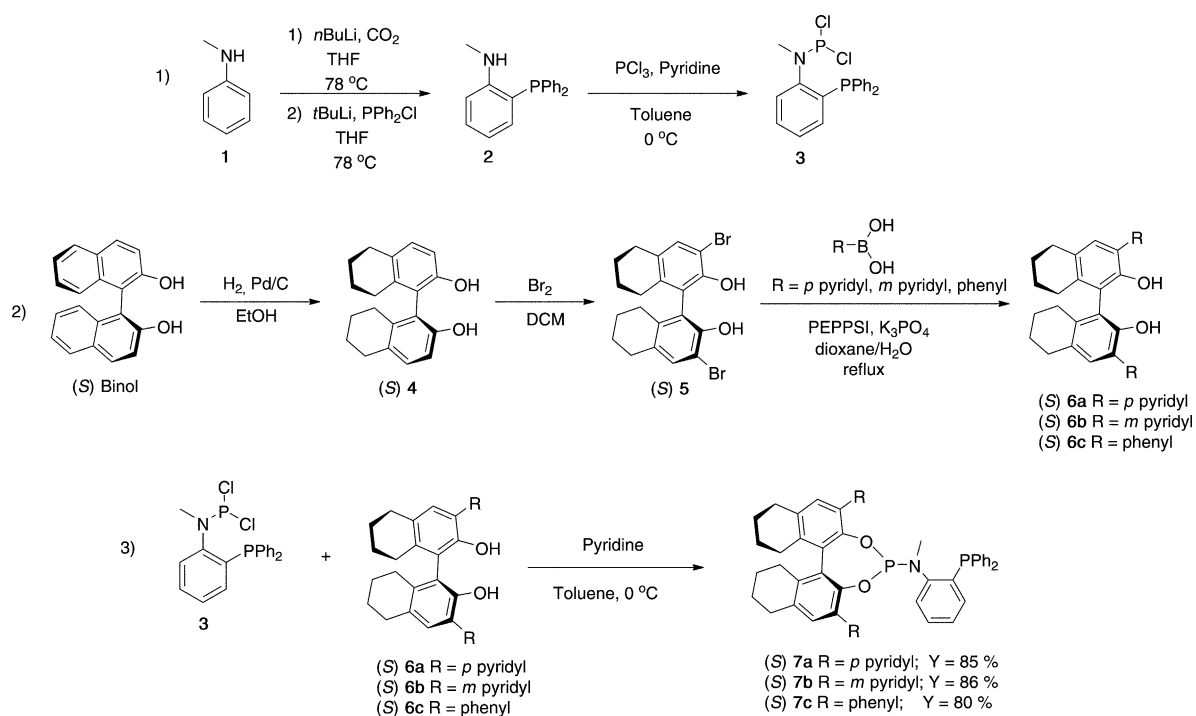


Figure 4. Supramolecular bidentate hybrid ligands.



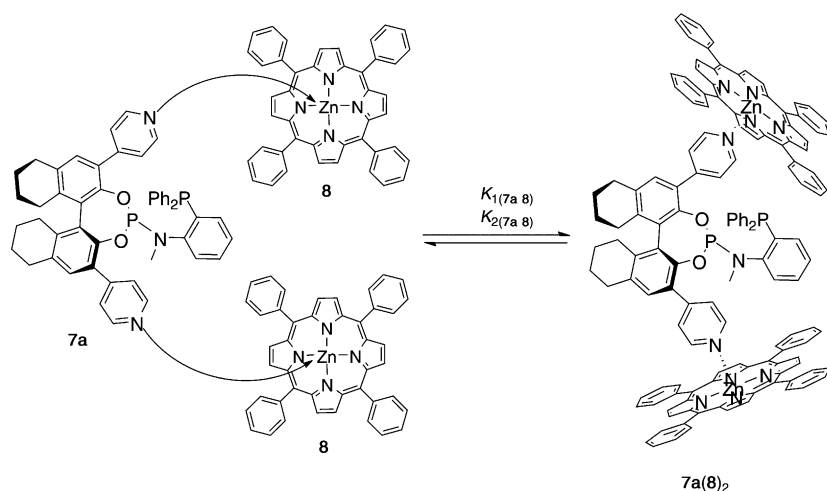
Scheme 1. Synthesis of chiral bidentate hybrid ligands (S)-7a-c.

presence of Pd/C.^[19] The diol **4** was selectively brominated at the 3,3'-positions to give product **5**.^[20] Suzuki coupling of **5** with the appropriate boronic acids provided compounds **6a-c**. Condensation of **3** with diols **6a-c** produced the hybrid ligands **7a-c** in good yields, up to 86% after flash column chromatography. All new compounds were fully characterised by ¹H, ¹³C and ³¹P NMR spectroscopy and by high-resolution mass spectrometry.

Coordination studies

UV/Vis titration: First, the coordination behaviour of ligands (S)-**7a** and (S)-**7b** towards zinc(II)-porphyrin **8** was investigated by using UV/Vis titration (Scheme 2). In the UV/Vis spectrum of **8**, a typical shift for the Q-bands of the porphyrin upon addition of **7a** or **7b** was observed and the binding constants were determined by fitting the titration curve using a mathematical model. Identical and independent binding constants were obtained for ligand **7a** ($K_{1(7a-8)} = K_{2(7a-8)} = 5.3 \times 10^3 \text{ M}^{-1}$) as well as for ligand **7b** ($K_{1(7b-8)} = K_{2(7b-8)} = 8.3 \times 10^3 \text{ M}^{-1}$).

It is known that the binding of zinc(II) templates occurs selectively through the nitrogen donors and, therefore, the phosphorus is available for coordination to the catalytically



Scheme 2. Assembly of ligand (*S*)-**7a** on *meso*-phenyl zinc(II)-porphyrin **8**.

active transition-metal centre. Hence, we next investigated the coordination of these bidentate hybrid ligands to the rhodium metal centre under hydroformylation conditions. The formation of the rhodium complexes for the ligands **7a(8)**₂, **7b(8)**₂ and (*S*)-**7a-c** were fully characterised by high-pressure (HP) NMR and HP IR spectroscopy.

High-pressure NMR experiments: Rhodium complexes were prepared for the HP NMR experiments by adding 1 equivalent of bidentate ligand to the metal precursor [Rh(acac)(CO)₂] in [D₈]toluene at 5 bar of syngas (H₂/CO, 1:1) pressure. According to these NMR experiments, displacement of the two carbon monoxide ligands by the bidentate ligand (P^{Ph}-P^{P-N}) resulted in the formation of the square planar complex [Rh(acac) P^{Ph}-P^{P-N}]. After an incubation time of 16 h at room temperature under these hydroformylation conditions, the expected hydridobiscarbonyl rhodium complex [RhH(CO)₂P^{Ph}-P^{P-N}] was formed. For unsymmetrical bidentate ligands, three different isomers can be formed, the eq-eq isomer, with both phosphorus donor atoms in equatorial position, and the two eq-ap isomers, in which either the phosphane or the phosphoramidite occupies the apical position, *trans* to the hydride (Figure 5).

Stable rhodium complexes were obtained for all the ligands, and in none of the experiments hydrolysis or oxidation of the ligands was observed. The chemical shifts of the phosphorus and hydride signals, as well as the coupling constants of the various complexes, measured under hydroformylation conditions, are shown in Table 1.

Ligand **7a(8)**₂ in the presence of the rhodium precursor gives rise to the formation of the square planar complex [Rh(acac)**7a(8)**₂]. This is evidenced by the HP ³¹P NMR spectroscopic analysis with two doublets centred, respectively, at δ = 46.5 and 146.0 ppm. After exposing [Rh(acac)**7a(8)**₂] to 5 bar syngas pressure, a new set of signals appeared in the HP ³¹P NMR spectrum, indicating conversion of the square planar precursor complex into the trigonal bipyramidal hydrido complex [Rh(H)(CO)₂**7a(8)**₂]. In

the HP ¹H NMR spectrum at high field a single hydride signal was detected. One of the hydride couplings was very large, which indicates that one of the phosphorus atoms is in a *trans* position to the hydride, implying formation of an eq-ap complex. The absence of the large coupling in the ¹H-³¹P NMR spectrum confirmed the *trans* relationship between one of the phosphorus atoms and the hydride. The ¹H-³¹P NMR spectrum displayed a doublet at δ = -10.1 ppm indicative of the coupling of a hy-

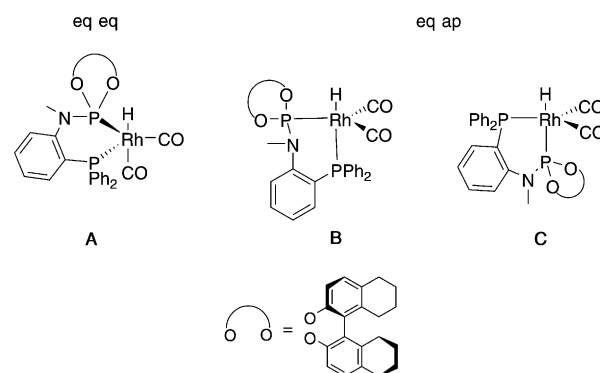


Figure 5. Structures of equatorial-equalatorial conformer **A** (eq-eq), and equatorial-apical conformers (eq-ap) **B** and **C** of the hydridobiscarbonyl rhodium complexes.

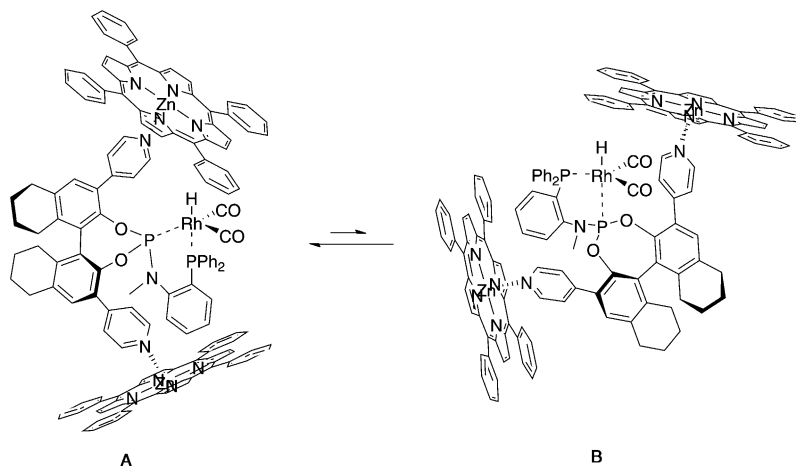
Table 1. ¹H and ³¹P high pressure NMR data for the [RhH(CO)₂P^{Ph}-P^{P-N}] complexes in [D₈]toluene.^[a]

Ligand	Hydride		Phosphane		Phosphoramidite				
	δ _{H-Rh}	J _{Rh-H}	δ _{P^{Ph}}	J _{P^{Ph}-Rh}	J _{P^{Ph}-H}	J _{P^{Ph}-P^N}	δ _{P^N}	J _{P^N-Rh}	J _{P^N-H}
7a(8) ₂	-10.1	11.0	30.5	89.1	120.3	62.5	166.2	234.2	- ^[b]
7a	-8.9	12.0	31.3	90.2	117.2	64.0	166.1	233.0	14.0
7b(8) ₂	-10.0	11.6	30.3	90.0	115.0	63.5	165.3	229.8	20.1
7b	-8.8	11.2	31.5	93.0	118.1	61.7	165.5	232.0	15.0
7c	-8.8	11.0	31.9	93.1	116.1	62.3	164.6	228.1	19.0

[a] Hydridobiscarbonyl rhodium complexes were generated in situ from [Rh(acac)(CO)₂] and the corresponding ligand after incubation at room temperature for 16 h under 5 bar H₂/CO in [D₈]toluene. [b] Value not detected due to small coupling constant.

dride with rhodium. The 2D ¹H-³¹P NMR spectrum supports the correlation of the single hydride signal in the ¹H NMR spectrum with the two doublet of doublets in the ³¹P NMR spectrum, providing further evidence for the formation of the hydridobiscarbonyl rhodium complex [Rh(H)(CO)₂**7a(8)**₂]. In addition, in the 2D ¹H-³¹P NMR spectrum, the cross peaks between the hydride signals and the doublet of doublets corresponding to the phosphane

ligand are more intense than the signal correlated to the phosphoramidite ligand, giving a clear indication that in the eq–ap complex the phosphane occupies the axial position, *trans* to the hydride and the phosphoramidite the equatorial position (Scheme 3, **A**). This is substantiated by the much larger coupling of the phosphane with the hydride than with the phosphoramidite.



Scheme 3. Structures of the eq–ap isomers **A** and **B** of the $[\text{Rh}(\text{H})(\text{CO})_2\cdot 7\mathbf{a}(\mathbf{8})_2]$ complex.

Similar results were obtained from the HP NMR investigations on the supramolecular ligand **7b(8)**₂ and ligands (*S*)-**7a–c**, with formation in all cases of a single eq–ap hydrido-biscarbonyl rhodium complex (Table 1). In these experiments the association of the zinc(II)-porphyrin **8** to ligands **7a** and **7b** does not change the ligand coordination mode, in contrast to what was observed for the monodentate analogue ligands.^[21]

In the initial coordination studies on the $[\text{Rh}(\text{H})(\text{CO})_2\text{-(R,S)-Binaphos}]$ complex, Nozaki and co-workers interpreted the HP NMR experiments as resulting from a single species with eq–ap coordination in which the phosphite ligand was *trans* to the hydride.^[7b] Further investigation by Jäkel, Nozaki and co-workers demonstrated that, at low temperature, both eq–ap conformers are present.^[7c] At room temperature these isomers are in rapid equilibrium and the spectra represent the average of these complexes. On the basis of these studies we decided to perform low-temperature HP ¹H and ³¹P NMR spectroscopic analysis of the $[\text{Rh}(\text{H})(\text{CO})_2\cdot 7\mathbf{a}(\mathbf{8})_2]$ complex to investigate the formation of the two eq–ap isomers. Upon lowering the temperature from 25 to –90 °C, the signals in both ¹H and ³¹P NMR spectra broaden but no new signals appeared. These experiments establish the exclusive formation of a single hydridobiscarbonyl rhodium active complex, in which the phosphane is mainly located *trans* to the hydride and the phosphoramidite is in the equatorial position (see the Supporting Information).

High-pressure IR experiments: In situ HP IR spectroscopy studies were then performed to study the formation of the

catalyst at concentrations identical to those used in catalysis experiments. We investigated the formation of the hydrido-biscarbonyl complexes with ligands **7a(8)**₂, **7a** and **7c**. The complexes were formed within 20 h at 40 °C and 20 bar H₂/CO in dichloromethane. In line with our HP NMR studies, only one set of carbonyl signals (symmetric and antisymmetric stretching modes) were observed in all cases, corresponding to the eq–ap isomer. The Rh–H vibration was not observed in the spectra, possibly because of overlap with one of the carbonyl signals.

In the $[\text{Rh}(\text{H})(\text{CO})_2\cdot 7\mathbf{a}]$ complex two peaks were detected in the carbonyl stretching region (2007.7 and 1958.6 cm^{–1}). In the presence of template **8** the $[\text{Rh}(\text{H})(\text{CO})_2\cdot 7\mathbf{a}(\mathbf{8})_2]$ complex is formed in which the two absorption bands are shifted to slightly higher wavenumbers (2011.1 and 1963.4 cm^{–1}; see the Supporting Information). In line with our previous findings using monodentate ligand analogues,^[21] coordination of the pyridyl leads to lower electron density on the rhodium, as indicated by the shift to higher wavenumbers. This implies a decrease of back-bonding to the CO molecules and, hence, faster CO dissociation and possibly an increase in the reaction rates. The IR spectrum corresponding to complex $[\text{Rh}(\text{H})(\text{CO})_2\cdot 7\mathbf{c}]$ also shows only one set of carbonyl signals (2005.1 and 1956.1 cm^{–1}) corresponding to the eq–ap complex (see the Supporting Information).

In all of the spectra, the carbonyl signals at higher wavenumbers have much lower intensity, suggesting possible distortion of the trigonal bipyramidal geometry in the Rh-hydrido complex. To obtain evidence for the formation of such a distorted structure, we carried out DFT calculations of complex $[\text{Rh}(\text{H})(\text{CO})_2\cdot 7\mathbf{c}]$. Indeed, the calculated structure of complex $[\text{Rh}(\text{H})(\text{CO})_2\cdot 7\mathbf{c}]$ reveal a distorted trigonal bipyramidal complex geometry (H–Rh–P^{Ph}, Angle = 172.87°). However, only a slight difference in the calculated Rh–CO and C–O bond lengths were observed (see the Supporting Information).

Asymmetric hydroformylation: The catalytic potential of the new bidentate ligands (*S*)-**7a–c** was evaluated in the Rh-catalysed asymmetric hydroformylation of styrene and *para*-substituted styrene derivatives. Ligands (*S*)-**7a–b** were applied in the presence and absence of template **8** to evaluate whether the effect of the supramolecular assemblies could possibly enhance the activity and selectivity of this catalytic transformation. We studied the performance of these ligands using styrene as a benchmark substrate under 20 bar of H₂/CO (1:1) at 25 °C (Table 4, entry 2). The supramolecular ligand **7a(8)**₂ gave higher conversion and slightly higher

Table 2. Asymmetric hydroformylation of styrene using ligand (*S*)-**7a–c** and template **8**.^[a]

Entry	Ligand	Conv. [%] ^[b]	b/l ^[c]	ee [%] ^[d]
1	7a (8) ₂	52	91:9	59 (<i>S</i>)
2	7a	5	95:5	51 (<i>S</i>)
3	7b (8) ₂	56	97:3	20 (<i>R</i>)
4	7b	3	99:1	52 (<i>S</i>)
5	7c	18	97:3	51 (<i>S</i>)
6	7c + 8	18	97:3	50 (<i>S</i>)

[a] Reagents and conditions: [Rh(acac)(CO)₂]=1 mM in toluene, ligand/rhodium=3, styrene/rhodium=200, 25 °C, 20 bar, 84 h. [b] Percentage conversion calculated on the basis of GC analysis. [c] Ratio of branched to linear aldehyde. [d] Enantiomeric ratio determined by chiral GC analysis (Supelco BETA DEX 225).

enantioselectivity compared with the nontemplated analogue **7a** (Table 2, entries 1 and 2). Ligand **7b**(**8**)₂ also gave higher conversion, albeit with lower and opposite enantioselectivity than ligand **7b** (Table 2, entries 3 and 4). Ligand **7c**, which was used as control because it lacks the pyridyl group, showed moderate conversion (Table 2, entry 5) and similar levels of enantioselection to that obtained with ligand **7a**. In the presence of template **8**, ligand **7c** displayed the same activity and selectivity, indicating that the zinc template does not directly affect the catalytic outcome of the reaction (Table 2, entry 6). In light of these preliminary results, in which only improvements in activity and small effects in selectivity were obtained in the presence of template **8**, we decided to investigate a small series of electronically and sterically different porphyrins. It is known that changing the substituents on the porphyrins alters the electron density on the pyridine moiety.^[22] Therefore, an effect in the electron density on the phosphorus atom can also be expected, which, in turn, might influence the catalysis outcome.

Variation of electronic properties of ligands 7a–b: In these studies we investigated the influence of different templates on the electronic and steric properties of ligands **7a–b**. Upon variation of the steric and electronic properties of the porphyrin building blocks^[23] (Figure 6), a series of new supramolecular ligands based on (*S*)-**7a–b** were evaluated in Rh-catalysed asymmetric hydroformylation of styrene (Table 3).

As is clear from the results presented in Table 3, the electronic properties of porphyrin templates have a distinct effect on the catalysis outcome. In particular, the assemblies of more electron-withdrawing zinc(II)-porphyrins on ligand **7a** leads to an increase in enantioselectivity up to 64% (Table 3, entries 1–5). A similar trend was obtained with supramolecular catalysts formed by ligand **7b** but with lower enantioselectivity (Table 3, entries 7–10). Interestingly, the highest enantioselectivity was obtained with the catalyst assemblies based on ruthenium(II) template **12** (Table 3, en-

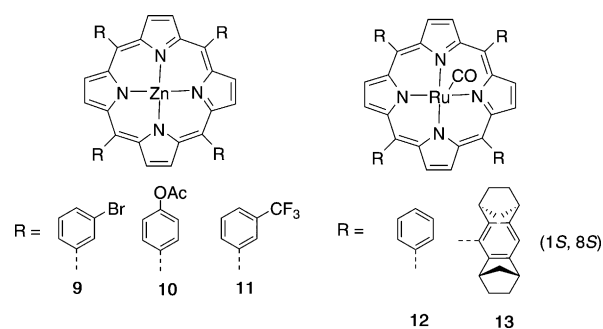


Figure 6. Zinc(II) and ruthenium(II) building blocks used in this study.

Table 3. Asymmetric hydroformylation of styrene; template screening.^[a]

Entry	Ligand	Template	Conv. [%] ^[b]	b/l ^[c]	ee [%] ^[d]
1	7a	8	52	91:9	59 (<i>S</i>)
2	7a	9	10	97:3	64 (<i>S</i>)
3	7a	10	10	98:2	40 (<i>S</i>)
4	7a	11	10	96:4	43 (<i>S</i>)
5	7a	12	9	99:1	72 (<i>S</i>)
6	7a	13	7	96:4	45 (<i>S</i>)
7	7b	9	11	97:3	26 (<i>R</i>)
8	7b	10	11	94:6	9 (<i>R</i>)
9	7b	11	10	95:5	10 (<i>R</i>)
10	7b	12	8	98:2	40 (<i>R</i>)
11	7b	13	8	98:2	8 (<i>R</i>)

[a] Reagents and conditions: [Rh(acac)(CO)₂]=1 mM in toluene, ligand/rhodium=3, styrene/rhodium=200, 25 °C, 20 bar, 84 h. [b] Percentage conversion calculated on the basis of GC analysis. [c] Ratio of branched to linear aldehyde. [d] Enantiomeric ratio determined by chiral GC analysis (Supelco BETA DEX 225).

tries 5 and 10), albeit with lower conversion than with template **8** (Table 3, entry 1 vs. entries 5 and 10). Ruthenium(II)-porphyrins bind pyridines with higher binding constants^[24] and the exchange between free and bonded species is slow on the NMR time-scale. These properties may be important for the development of more selective catalysts. Similar results were reported for the assembly of tris-3-pyridylphosphine with ruthenium(II)-porphyrin **12**, in which the hydroformylation of 1-octene delivers higher selectivity but lower activity compared with the assembly based on zinc(II)-porphyrin (**8**).^[25] Changes in the steric bulk of template **12**, using, for example, template **13**, leads to similar activity and regioselectivity, but lower enantioselectivity (Table 3, entries 6 and 11). This can be explained by a match/mismatch effect due to the presence of multiple stereocentres. Because the other diastereomer was not available, we have not further studied this effect.

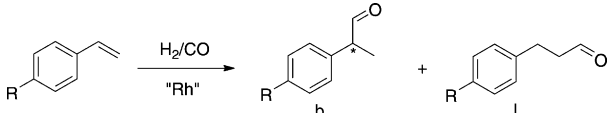
By using these new supramolecular bidentate systems we are able to fine-tune the properties of the ligands and thus influence the catalytic outcome of the reaction, by just changing the properties of the supramolecular templates. This is in contrast to our earlier findings employing monodentate analogues of ligands **7a–b**,^[21] in which the catalytic properties of the supramolecular catalysts were not influenced by the properties of zinc templates, but instead were

associated with the change in the coordination mode of the ligand.

Asymmetric hydroformylation of *para*-substituted styrenes: Having established **12** as the best template, we investigated the substrate scope, studying the performance of supramolecular ligands **7a(12)₂** and **7b(12)₂** as well as the control ligand **7a–c** in the AHF of *para*-substituted styrenes.

The catalytic results obtained by employing the supramolecular ligand **7a(12)₂** displayed a branched isomer selectivity that increases with more electron-withdrawing substrates (Table 4, entries 1 and 3 vs. entry 5). A similar trend in regioselectivity was observed for the nontemplated ligand **7a** (Table 4, entries 2, 4 and 6). Interestingly, higher enantioselectivities were obtained with the supramolecular assemblies (Table 4, entries 1, 3 and 5) with *ee* values up to 82% compared with the nontemplated ligand. The nontemplated ligand gives, however, slightly higher conversions (Table 4, entries 2, 4 and 6).

Table 4. Asymmetric hydroformylation of styrene derivatives using ligand (*S*)-**7a** and template **12**.^[a]



Entry	R	Template	Conv. [%] ^[b]	b/l ^[c]	<i>ee</i> [%] ^[d]
1	OCH ₃	12	10	90:10	82 (<i>S</i>)
2	OCH ₃	–	21	91:9	18 (<i>S</i>)
3	CH ₃	12	16	95:5	80 (<i>S</i>)
4	CH ₃	–	22	92:8	15 (<i>S</i>)
5	Cl	12	12	99:1	66 (<i>S</i>)
6	Cl	–	18	99:1	13 (<i>S</i>)

[a] Reagents and conditions: [Rh(acac)(CO)₂]=1 mM in toluene, ligand/rhodium=3, *p*-styrene/rhodium=200, 25 °C, 20 bar, 84 h. [b] Percentage conversion calculated on the basis of GC analysis. [c] Ratio of branched to linear aldehyde. [d] Enantiomeric ratio determined by chiral GC analysis (Supelco BETA DEX 225).

Interestingly, for ligand **7b**, which is similar to ligand **7a**, but with a *m*-pyridyl group instead of a *p*-pyridyl, we found the reverse effect. Supramolecular bidentate ligand **7b(12)₂** displayed lower selectivity compared with the nontemplated analogue **7b** (Table 5, entries 1, 3 and 5 vs. entries 2, 4 and 6). Surprisingly, supramolecular ligand **7b(12)₂** induced opposite enantioselectivity, with preferred formation of the *R* enantiomer (Table 5, entries 1, 3, and 5). It should be noted that all ligands have the same absolute configuration of the 8H-Binol moiety. Marginal changes in regioselectivity were obtained with more electron-withdrawing substrates.

Control experiments using ligand **7c**, which has phenyl groups instead of pyridyls, show that the catalyst-induced regioselectivity was independent of the electronic nature of the substrate. The enantioselectivity is slightly higher than that induced by **7a**, and much lower than that of supramolecular ligand **7a(12)₂** (Table 6, entries 1–3).

Table 5. Asymmetric hydroformylation of styrene derivatives using ligand (*S*)-**7b** and template **12**.^[a]

Entry	R	Template	Conv. [%] ^[b]	b/l ^[c]	<i>ee</i> [%] ^[d]
1	OCH ₃	12	9	92:8	37 (<i>R</i>)
2	OCH ₃	–	18	92:8	60 (<i>S</i>)
3	CH ₃	12	13	99:1	32 (<i>R</i>)
4	CH ₃	–	16	98:2	69 (<i>S</i>)
5	Cl	12	13	99:1	17 (<i>R</i>)
6	Cl	–	12	99:1	30 (<i>S</i>)

[a] Reagents and conditions: [Rh(acac)(CO)₂]=1 mM in toluene, ligand/rhodium=3, *p*-styrene/rhodium=200, 25 °C, 20 bar, 84 h. [b] Percentage conversion calculated on the basis of GC analysis. [c] Ratio of branched to linear aldehyde. [d] Enantiomeric ratio determined by chiral GC analysis (Supelco BETA DEX 225).

Table 6. Asymmetric hydroformylation of styrene derivatives using ligand (*S*)-**7c**.^[a]

Entry	R	Conv. [%] ^[b]	b/l ^[c]	<i>ee</i> [%] ^[d]
1	OCH ₃	15	93:7	26 (<i>S</i>)
2	CH ₃	10	93:7	38 (<i>S</i>)
3	Cl	25	94:6	30 (<i>S</i>)

[a] Reagents and conditions: [Rh(acac)(CO)₂]=1 mM in toluene, ligand/rhodium=3, *p*-styrene/rhodium=200, 25 °C, 20 bar, 84 h. [b] Percentage conversion calculated on the basis of GC analysis. [c] Ratio of branched to linear aldehyde. [d] Enantiomeric ratio determined by chiral GC analysis (Supelco BETA DEX 225).

Interestingly, a correlation between enantioselectivity and the Hammett constants^[26] (substrate σ value) was observed for the supramolecular ligands **7a(12)₂** and **7b(12)₂**. Plotting the *ee* values against the Hammett constants of the substrates (*p*-methoxystyrene -0.27 , *p*-methylstyrene -0.17 , styrene 0, *p*-chlorostyrene $+0.23$), a decrease of *ee* was obtained when σ increased (Figure 7). On the other hand, no

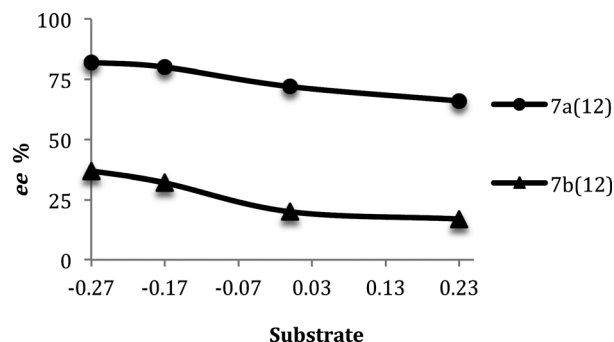


Figure 7. Plot of the *ee* values versus Hammett constants σ for ligands **7a(12)₂** and **7b(12)₂**.

clear correlation between enantioselectivity and substrate electronics was observed for ligands **7a–c** (Figure 8). In a recent publication, our group has reported on phosphane-phosphite ligands in the AHF of electronically different styrene derivatives.^[27] A trend between the electronic properties of the substrate and the orientation of the phenyl groups of P-ligands was observed, with the conclusion that aryl–aryl (π – π) interactions between substrate and ligands might take

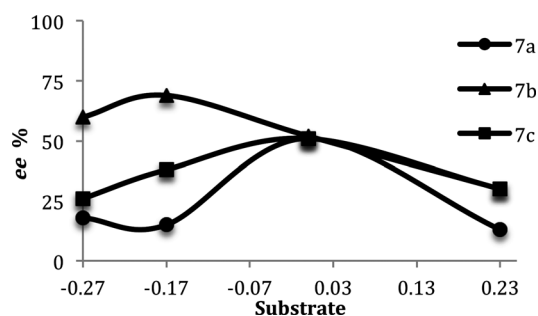


Figure 8. Plot of the *ee* values versus Hammett constants σ for ligands **7a–c**.

place, hence, influencing the selectivity of the reaction. This may indeed also occur in our system, in which the substrate and the phenyl groups of the porphyrin could interact through weak interactions, and therefore influence the enantioselectivity.

Next, we decided to perform the catalysis at higher temperature (40 °C) with the aim of increasing the conversion of ligands **7a(12)₂**, **7b(12)₂**, **7a** and **7b**. As shown in Table 7, all the ligands provided catalysts that gave full conversion at

Table 7. Asymmetric hydroformylation of styrene derivatives.^[a]

Entry	R	Ligand	Conv. [%] ^[b]	b/l ^[c]	<i>ee</i> [%] ^[d]	<i>ee</i> [%] ^[e]
1	OCH ₃	7a(12)₂	99	95:5	51 (<i>S</i>)	82 (<i>S</i>)
2	OCH ₃	7a	87	95:5	10 (<i>S</i>)	18 (<i>S</i>)
3	CH ₃	7a(12)₂	98	96:4	42 (<i>S</i>)	80 (<i>S</i>)
4	CH ₃	7a	89	96:4	15 (<i>S</i>)	15 (<i>S</i>)
5	H	7a(12)₂	95	92:8	12 (<i>S</i>)	59 (<i>S</i>)
6	H	7a	> 99	99:1	32 (<i>S</i>)	51 (<i>S</i>)
7	Cl	7a(12)₂	99	97:3	2 (<i>S</i>)	66 (<i>S</i>)
8	Cl	7a	> 99	98:2	11 (<i>S</i>)	13 (<i>S</i>)
9	OCH ₃	7b(12)₂	99	94:6	11 (<i>R</i>)	37 (<i>R</i>)
10	OCH ₃	7b	99	93:7	18 (<i>S</i>)	60 (<i>S</i>)
11	CH ₃	7b(12)₂	> 99	99:1	16 (<i>R</i>)	32 (<i>R</i>)
12	CH ₃	7b	> 99	99:1	23 (<i>S</i>)	69 (<i>S</i>)
13	H	7b(12)₂	> 99	94:6	12 (<i>R</i>)	20 (<i>R</i>)
14	H	7b	> 99	94:6	18 (<i>S</i>)	52 (<i>S</i>)
15	Cl	7b(12)₂	> 99	96:4	3 (<i>R</i>)	17 (<i>R</i>)
16	Cl	7b	> 99	97:3	7 (<i>S</i>)	30 (<i>S</i>)
17 ^[f]	H	7a(12)₂	14	99:1	69 (<i>S</i>)	

[a] Reagents and conditions: [Rh(acac)(CO)₂]=1 mM in toluene, ligand/rhodium=3, *p*-styrene/rhodium=200, 40 °C, 20 bar, 84 h. [b] Percentage conversion calculated on the basis of GC analysis. [c] Ratio of branched to linear aldehyde. [d] Enantiomeric ratio determined by chiral GC analysis (Supelco BETA DEX 225). [e] *ee* at 25 °C. [f] Incubation at 40 °C and catalysis reaction at 25 °C.

40 °C but at the expense of regio- and enantioselectivity. With supramolecular ligand **7a(12)₂**, a similar trend in enantioselectivity as was observed at 25 °C, with a decrease in *ee* when the substrate σ value increases (Table 7, entries 1, 3, 5 and 7). Generally, the enantioselectivity is lower at higher temperature, but, remarkably, this is more pronounced in some reactions involving the supramolecular ligands. For example, the *ee* becomes even lower than the corresponding nontemplate analogue (Table 7, entry 5 vs. 6, entry 7 vs. 8).

This could be related to the presence of multiple active isomers of the supramolecular catalyst, which have different selectivities. Incubation of the catalyst at 40 °C for 18 h and then reaction at lower temperature (25 °C) did not result in higher conversion (Table 7, entry 17).

Conclusion

We report here the synthesis of a new class of supramolecular hybrid bidentate ligands and their application in AHF reactions. We investigated the coordination behaviour of these ligands with zinc(II) template **8** as well as to rhodium complexes under catalytically relevant conditions by using high pressure NMR and IR spectroscopy. These studies revealed the formation of a single rhodium bis-carbonyl hydrido complex in which the phosphane ligand resides on the axial position and the phosphoramidite ligand in the equatorial position. In the rhodium-catalysed asymmetric hydroformylation of styrene, modification of steric and electronic functionalities on the zinc(II) and ruthenium(II) templates have been shown to have a significant influence on the activity and selectivity of the reaction. A notable improvement in enantioselectivity was obtained with the supramolecular ligand **7a(12)₂** and ligands based on **7a** with zinc(II) templates functionalised with electron-withdrawing groups. Application of **7a(12)₂** in the AHF of styrene and *para*-substituted styrene derivatives thereof shows higher enantiocontrol compared to the nontemplated analogue ligands. This work demonstrates the potential of the supramolecular strategy in tailoring key catalyst properties such as activity and selectivity by using sterically and electronically different templates.

Experimental Section

Unless stated otherwise, reactions were carried out under an atmosphere of argon using standard Schlenk techniques. THF was distilled from sodium benzophenone ketyl; CH₂Cl₂ was distilled from CaH₂ and toluene was distilled from sodium under nitrogen. With the exception of the compounds given below, all reagents were purchased from commercial suppliers and used without further purification.

NMR spectra (¹H, ³¹P and ¹³C) were measured with a Bruker DRX 400 MHz or Inova 500 MHz spectrometer; CDCl₃ was used as a solvent, if not further specified. High-resolution mass spectra were recorded with a JEOL JMS SX/SX102A four sector mass spectrometer; for FAB-MS, 3-nitrobenzyl alcohol was used as matrix. UV/Vis spectroscopy experiments were performed with a Cary UV/Vis System. Gas chromatographic analyses were performed with a Shimadzu GC-17A apparatus (split/splitless injector, J&W Scientific, DB-1J&W 30 m column, film thickness 3.0 μm, carrier gas 70 kPa He, FID Detector). Chiral GC separations were conducted with an Interscience HR GC apparatus with a Supelco β-dex 225 (0.25 mm × 30 m) capillary column.

The following compounds were synthesised according to published procedures: 2-(diphenylphosphino)-*N*-methylaniline (**2**),^[18] (*S*)-5,6,7,8,5,6,7,8-octahydro-(1,1'-binaphthalene)-2,2'-diol (**4**),^[19] (*S*)-3,3'-dibromo-5,6,7,8,5',6',7',8'-octahydro-(1,1'-binaphthalene)-2,2'-diol (**5**),^[20] zinc(II)-porphyrins **8–11**.^[22] Zinc(II)-porphyrin **13** was kindly donated by the group of A. Berkessel, Institute of Organic Chemistry, University of Köln, Germany. Details of the synthesis used to obtain (*S*)-**6a–c** were reported in a previous publication.^[21]

Synthesis of 1,1-dichloro-*N*-(2-(diphenylphosphino)phenyl)-*N*-methylphosphinamine (3): In a flame-dried Schlenk, distilled PCl_3 (0.22 mL, 2.6 mmol) was added dropwise at 0°C to a solution of 2-(diphenylphosphino)-*N*-methylaniline (500 mg, 1.7 mmol), and Et_3N (0.24 mL, 1.7 mmol) in toluene (8.5 mL). The pale-yellow slurry was allowed to warm to RT and then heated to 75°C for 16 h. The reaction mixture was cooled to RT and the formation of product was monitored by ^{31}P NMR spectroscopic analysis. The solvent and the residual PCl_3 was removed in vacuum and the resulting solid was used for the next step without any further purification.

General procedure for the preparation of ligands (S)-7a-c: In a flame-dried Schlenk flask, compound (S)-6a-c (1.2 mmol), DMAP (10 mol %) and pyridine (0.1 mL, 1.3 mmol) were dissolved in anhydrous THF (4 mL). The resulting solution was cooled to 0°C and phosphorodichloridite **3** (467 mg, 1.2 mmol) in THF (2 mL) was added. The reaction mixture was stirred overnight and warmed to RT. The resulting pale-yellow solution was evaporated to dryness, and the resulting residue was purified by flash column chromatography (silica gel; hexanes/ CH_2Cl_2 , 1:1 to hexanes/ CH_2Cl_2 / Et_3N , 1:1:0.2).

Ligand (S)-7a: Yield: 85%; white foam; ^1H NMR (400 MHz, CDCl_3): $\delta = 8.7$ (d, $J = 5.7$ Hz, 4H), 8.5 (d, $J = 5.7$ Hz, 2H), 7.7 (m, 7H), 7.0 (m, 7H), 6.8 (s, 2H), 2.9 (m, 4H), 2.7 (m, 2H), 2.4 (m, 2H), 1.7 (m, 8H), 1.6 ppm (s, 3H); ^{13}C NMR (101 MHz): $\delta = 150.0$ (CH), 149.6 (CH), 148.5 (C), 146.2 (C), 145.4 (C), 138.9 (C), 138.6 (C), 135.1 (CH), 134.5 (C), 133.7 (C), 133.7 (CH), 133.6 (CH), 133.4 (CH), 133.2 (CH), 130.4 (CH), 130.2 (C), 129.9 (CH), 129.4 (C), 129.0 (CH), 128.9 (CH), 128.7 (CH), 128.6 (CH), 128.5 (CH), 128.4 (CH), 128.3 (CH), 128.2 (CH), 128.1 (CH), 127.9 (C), 126.9 (CH), 124.9 (CH), 124.5 (CH), 35.6 (CH₃), 29.2 (CH₂), 29.1 (CH₂), 28.0 (CH₂), 27.7 (CH₂), 22.7 (CH₂), 22.7 (CH₂), 22.6 (CH₂), 22.5 ppm (CH₂); ^{31}P NMR (162 MHz): $\delta = 139.5$ (d, $J = 55$ Hz), -14.5 ppm (d, $J = 55$ Hz); HRMS (FAB+): m/z calcd for $\text{C}_{49}\text{H}_{43}\text{N}_3\text{O}_2\text{P}_2$: 768.2909 [$M+H^+$]; found: 768.2906.

Ligand (S)-7b: Yield: 86%; white foam; ^1H NMR (400 MHz, CDCl_3): $\delta = 8.9$ (s, 1H), 8.8 (s, 1H), 8.6 (m, 1H), 8.2 (m, 1H), 8.1 (m, 2H), 7.3 (m, 2H), 7.1 (m, 6H), 6.9 (m, 8H), 6.7 (m, 2H), 2.9 (m, 4H), 2.7 (m, 2H), 2.4 (m, 2H), 1.7 (m, 8H), 1.6 ppm (s, 3H); ^{13}C NMR (101 MHz): $\delta = 150.3$ (CH), 150.0 (CH), 148.3 (C), 147.9 (CH), 147.8 (CH), 145.7 (C), 138.2 (C), 137.8 (C), 137.9 (CH), 137.4 (CH), 134.8 (CH), 134.6 (C), 134.4 (C), 134.0 (CH), 133.8 (CH), 133.6 (C), 133.5 (C), 133.4 (CH), 133.2 (CH), 130.7 (CH), 130.3 (C), 129.9 (CH), 129.6 (C), 128.9 (C), 128.2 (CH), 128.1 (CH), 128.0 (CH), 127.9 (CH), 127.8 (CH), 126.6 (CH), 123.4 (CH), 123.2 (CH), 35.6 (CH₃), 29.2 (CH₂), 29.2 (CH₂), 28.0 (CH₂), 27.7 (CH₂), 22.8 (CH₂), 22.7 (CH₂), 22.6 (CH₂), 22.5 ppm (CH₂); ^{31}P NMR (162 MHz): $\delta = 138.5$ (d, $J = 57$ Hz), -14.5 ppm (d, $J = 57$ Hz); HRMS (FAB+): m/z calcd for $\text{C}_{49}\text{H}_{43}\text{N}_3\text{O}_2\text{P}_2$: 768.2909 [$M+H^+$]; found: 768.2906.

Ligand (S)-7c: Yield: 80%; white foam; ^1H NMR (400 MHz, CDCl_3): $\delta = 7.7$ (m, 4H), 7.4 (m, 4H), 7.3 (m, 2H), 7.2 (m, 6H), 7.1 (m, 4H), 6.9 (m, 4H), 6.8 (m, 2H), 2.9 (m, 4H), 2.7 (m, 2H), 2.4 (m, 2H), 1.8 (m, 8H), 1.6 ppm (s, 3H); ^{13}C NMR (101 MHz): $\delta = 138.8$ (C), 137.9 (C), 137.0 (C), 134.5 (CH), 134.1 (CH), 133.8 (CH), 133.7 (C), 133.6 (CH), 133.5 (CH), 132.9 (C), 130.8 (CH), 130.7 (C), 130.2 (CH), 130.0 (CH), 129.6 (CH), 128.4 (CH), 128.2 (CH), 128.1 (CH), 128.0 (CH), 127.9 (CH), 127.8 (CH), 126.8 (CH), 126.6 (CH), 30.3 (CH₃), 29.3 (CH₂), 29.2 (CH₂), 27.9 (CH₂), 27.7 (CH₂), 23.0 (CH₂), 22.9 (CH₂), 22.8 (CH₂), 22.5 ppm (CH₂); ^{31}P NMR (162 MHz): $\delta = 133.2$ (d, $J = 47$ Hz), -20.5 ppm (d, $J = 47$ Hz); HRMS (FAB+): m/z calcd for $\text{C}_{51}\text{H}_{45}\text{NO}_2\text{P}_2$: 766.2926 [$M+H^+$]; found: 766.3012.

General procedure for the rhodium-catalysed hydroformylation reactions: A typical experiment was carried out in a stainless steel autoclave (150 mL) charged with an insert that was suitable for 14 reaction vessels (equipped with Teflon mini stirring bar) for performing parallel reactions. Each vial was charged with zinc(II)-template (6 μmol , 6 equiv), ligand (3 μmol , 3 equiv), $[\text{Rh}(\text{acac})\text{CO}_2]$ (1 μmol), substrate (200 μmol) and toluene (1 mL). The substrate was filtered over basic alumina to remove possible peroxide impurities. The toluene was distilled from sodium prior to use. Before starting the catalysis, the charged autoclave was purged three times with 10 bar syngas ($\text{H}_2/\text{CO} = 1:1$) and then pressurized to

20 bar. After the catalytic reaction, the pressure was reduced to 1.0 bar and a few drops of tri-*n*-butyl-phosphite were added to each reaction vessel to prevent any further reaction. The reaction mixtures were not filtered over basic alumina to remove catalyst residues because filtration may cause retention of the aldehydes and thus influence the results of the GC analysis. The mixtures were diluted with CH_2Cl_2 for GC analysis.

Chiral GC data for hydroformylation products: The *ee* values were calculated by chiral GC analysis (Supelco BETA DEX 225). Initial temperature = 100°C for 5 min, then 4°C min^{-1} to 160°C .

Styrene $t_R = 4.35$ min, t_R (S) = 11.55 min and t_R (R) = 11.78 min.

p-Me-Styrene $t_R = 6.96$ min, t_R (S) = 14.42 min and t_R (R) = 14.55 min.

p-OMe-Styrene $t_R = 13.76$ min, t_R (S) = 18.92 min and t_R (R) = 18.98 min.

p-Cl-Styrene $t_R = 9.55$ min, t_R (S) = 18.34 min and t_R (R) = 18.47 min.

Preparation of the hydride complexes for high-pressure NMR spectroscopy: A solution of ligand (S)-7a-c (1 equiv), template **8** (2 equiv), and $[\text{Rh}(\text{acac})\text{CO}_2]$ in $[\text{D}_8]$ toluene (20 mm) was stirred at 40°C for 3 h. After this time, the mixture was transferred into a 5 mm HP NMR tube, pressurized with 5 bar syngas H_2/CO 1:1 (5 bar) at RT for 16 h and the high-pressure NMR spectra were recorded.

Preparation of the hydride complexes for high-pressure IR spectroscopy: High-pressure IR experiments were performed with an SS-316 50 mL autoclave equipped with IRTRAN windows (ZnS, transparent above 700 cm^{-1} , $\phi = 10$ mm, optical path length = 0.4 mm), a mechanical stirrer, temperature controller, and a pressure device. In a typical experiment, the high-pressure IR autoclave was filled with (S)-7a-c (0.03 mmol), template **8** (0.06 mmol) and CH_2Cl_2 (13 mL). The autoclave was purged three times with 15 bar H_2/CO (1:1) and pressurized to 20 bar. The antichamber was charged with a solution of $[\text{Rh}(\text{acac})\text{CO}_2]$ (0.01 mmol) in CH_2Cl_2 (1 mL) and pressurized to 30 bar. The HP-IR autoclave was placed into a Nicolet 510 FTIR spectrometer and the temperature was set to 40°C . When the desired temperature was reached, the antichamber was opened and the catalyst precursor was injected into the solution. A series of IR spectra was recorded for 16 h while the samples were stirred.

Acknowledgements

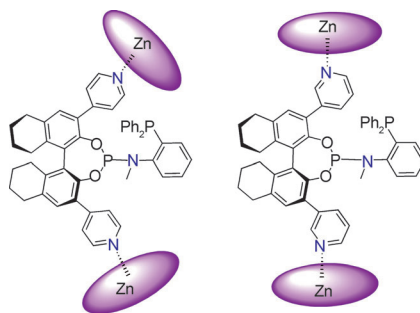
Pawel Dydio is kindly acknowledged for performing the DFT calculations. This work was financially supported by the National Research School Combination Chemistry (NRSC-C).

- [1] a) P. W. N. M. van Leeuwen, C. Claver, in *Rhodium-Catalysed Hydroformylation*, Kluwer Academic Publishers, Dordrecht **2000**; b) B. Breit, W. Seiche, *Synthesis* **2001**, 1–36; c) P. W. N. M. van Leeuwen, *Homogeneous Catalysis, Understanding the Art*, Kluwer Academic Publishers, Dordrecht **2004**.
- [2] a) F. Agbossou, J. F. Carpentier, A. Mortreaux, *Chem. Rev.* **1995**, 95, 2485–2506; b) J. Klosin, C. R. Landis, *Acc. Chem. Res.* **2007**, 40, 1251–1259; c) A. Gual, C. Godard, S. Castillón, C. Claver, *Tetrahedron: Asymmetry* **2010**, 21, 1135–1146.
- [3] J. E. Babin, G. T. Whiteker, PCT Int. Appl. WO 9303839, **1993**.
- [4] a) C. J. Cobley, K. Gardner, J. Klosin, C. Praquin, C. Hill, G. T. Whiteker, A. Zanotti-Gerosa, J. L. Petersen, K. A. Abboud, *J. Org. Chem.* **2004**, 69, 4031–4040; b) C. J. Cobley, J. Klosin, C. Qin, G. T. Whiteker, *Org. Lett.* **2004**, 6, 3277–3280.
- [5] a) S. Breeden, M. Wills, *J. Org. Chem.* **1999**, 64, 9735–9738; b) S. Breeden, D. J. Cole-Hamilton, D. F. Foster, G. J. Schwarz, M. Wills, *Angew. Chem.* **2000**, 112, 4272–4274; *Angew. Chem. Int. Ed.* **2000**, 39, 4106–4108.
- [6] a) C. R. Landis, W. C. Jin, J. S. Owen, T. P. Clark, *Angew. Chem.* **2001**, 113, 3540–3542; *Angew. Chem. Int. Ed.* **2001**, 40, 3432–3434; b) T. P. Clark, C. R. Landis, S. L. Freed, J. Klosin, K. A. Abboud, *J. Am. Chem. Soc.* **2005**, 127, 5040–5042; c) A. L. Watkins, B. G. Hashiguchi, C. R. Landis, *Org. Lett.* **2008**, 10, 4553–4556.

- [7] a) N. Sakai, K. Nozaki, H. Takaya, *J. Chem. Soc. Chem. Commun.* **1994**, 395–396; b) K. Nozaki, N. Sakai, T. Nanno, T. Higashijima, S. Mano, T. Horiuchi, H. Takaya, *J. Am. Chem. Soc.* **1997**, *119*, 4413–4423; c) D. A. Castillo Molina, C. P. Casey, I. Müller, K. Nozaki, C. Jäkel, *Organometallics* **2010**, *29*, 3362–3367.
- [8] a) Y. Yan, X. Zhang, *J. Am. Chem. Soc.* **2006**, *128*, 7198–7202; b) X. Zhang, B. Cao, Y. Yan, S. Yu, B. Ji, *Chem. Eur. J.* **2010**, *16*, 871–877.
- [9] a) S. Deerenberg, P. C. J. Kamer, P. W. N. M. van Leeuwen, *Organometallics* **2000**, *19*, 2065–2072; b) S. Deerenberg, O. Pamies, M. Dieguez, C. Claver, P. C. J. Kamer, P. W. N. M. van Leeuwen, *J. Org. Chem.* **2001**, *66*, 7626–7631.
- [10] M. Diéguez, O. Pamies, A. Ruiz, S. Castillon, C. Claver, *Chem. Eur. J.* **2001**, *7*, 3086–3094.
- [11] M. Rubio, A. Suarez, E. Alvarez, C. Bianchini, W. Oberhauser, M. Peruzzini, A. Pizzano, *Organometallics* **2007**, *26*, 6428–6436.
- [12] G. M. Noonan, J. A. Fuentes, C. J. Cobley, M. L. Clarke, *Angew. Chem.* **2012**, *124*, 2527–2530; *Angew. Chem. Int. Ed.* **2012**, *51*, 2477–2480.
- [13] T. Robert, Z. Abiri, J. Wassenaar, A. J. Sandee, S. Romanski, J. M. Neudorfl, H. G. Schmalz, J. N. H. Reek, *Organometallics* **2010**, *29*, 478–483.
- [14] a) J. Wassenaar, B. de Bruin, J. N. H. Reek, *Organometallics* **2010**, *29*, 2767–2776; b) S. H. Chikkali, R. Bellini, G. Berthon-Gelloz, J. I. van der Vlugt, B. de Bruin, J. N. Reek, *Chem. Commun.* **2010**, *46*, 1244–1246; c) S. H. Chikkali, R. Bellini, B. de Bruin, J. I. van der Vlugt, J. N. H. Reek, *J. Am. Chem. Soc.* **2012**, *134*, 6607–6616.
- [15] a) B. Breit, *Angew. Chem.* **2005**, *117*, 6976–6986; *Angew. Chem. Int. Ed.* **2005**, *44*, 6816–6825; b) M. J. Wilkinson, P. W. N. M. van Leeuwen, J. N. H. Reek, *Org. Biomol. Chem.* **2005**, *3*, 2371–2383; c) A. J. Sandee, J. N. H. Reek, *Dalton Trans.* **2006**, 3385–3391; d) G. Gasparini, M. Dal Molin, L. J. Prins, *Eur. J. Org. Chem.* **2010**, 2429–2440; e) S. Carboni, C. Gennari, L. Pignataro, U. Piarulli, *Dalton Trans.* **2011**, *40*, 4355–4373; f) J. Meeuwissen, J. N. H. Reek, *Nature Chem.* **2010**, *2*, 615–621; g) P. W. N. M. van Leeuwen, *Supramolecular Catalysis*, Wiley-VCH, Weinheim, **2008**; h) P. E. Goudriaan, P. W. N. M. van Leeuwen, M. N. Birkholz, J. N. H. Reek, *Eur. J. Inorg. Chem.* **2008**, 2939–2958; i) R. Bellini, J. I. van der Vlugt, J. N. H. Reek, *Isr. J. Chem.* **2012**, *52*, 613–629.
- [16] a) M. Kuil, P. E. Goudriaan, P. W. N. M. van Leeuwen, J. N. H. Reek, *Chem. Commun.* **2006**, 4679–4681; b) M. Kuil, P. E. Goudriaan, A. W. Kleij, D. M. Tooke, A. L. Spek, P. W. N. M. van Leeuwen, J. N. H. Reek, *Dalton Trans.* **2007**, 2311–2320.
- [17] a) V. F. Slagt, M. Röder, P. C. J. Kamer, P. W. N. M. van Leeuwen, J. N. H. Reek, *J. Am. Chem. Soc.* **2004**, *126*, 4056–4057; b) P. E. Goudriaan, M. Kuil, X.-B. Jiang, P. W. N. M. van Leeuwen, J. N. H. Reek, *Dalton Trans.* **2009**, 1801–1805.
- [18] A. B. van Oort, P. H. M. Budzelaar, J. H. G. Frijns, *J. Organomet. Chem.* **1990**, *396*, 33–47.
- [19] A. Korostylev, V. I. Tararov, C. Fischer, A. Monsees, A. Borner, *J. Org. Chem.* **2004**, *69*, 3220–3222.
- [20] M. Bartoszek, M. Beller, J. Deutsch, M. Klawonn, A. Kockritz, N. Nemati, A. Pews-Davtyan, *Tetrahedron* **2008**, *64*, 1316–1322.
- [21] a) R. Bellini, S. H. Chikkali, G. Berthon-Gelloz, J. N. H. Reek, *Angew. Chem.* **2011**, *123*, 7480–7483; *Angew. Chem. Int. Ed.* **2011**, *50*, 7342–7345; b) R. Bellini, J. N. H. Reek, *Chem. Eur. J.* **2012**, *18*, 7091–7099.
- [22] C. T. Brewer, G. Brewer, *Inorg. Chim. Acta* **1986**, *111*, 25–30.
- [23] a) A. D. Adler, F. R. Longo, J. D. Finarelli, J. D. Goldmacher, J. Assour, L. Korsakoff, *J. Org. Chem.* **1967**, *32*, 476; b) A. D. Adler, F. R. Longo, F. Kampas, J. Kim, *J. Inorg. Nucl. Chem.* **1970**, *32*, 2443–2445.
- [24] a) K. M. Kadish, D. Chang, *Inorg. Chem.* **1982**, *21*, 3614–3618; b) D. P. Rillema, J. K. Nagle, L. F. Barringer, Jr., T. J. Meyer, *J. Am. Chem. Soc.* **1981**, *103*, 56–62.
- [25] V. F. Slagt, P. C. J. Kamer, P. W. N. M. van Leeuwen, J. N. H. Reek, *J. Am. Chem. Soc.* **2004**, *126*, 1526–1536.
- [26] C. Hansch, A. Leo, R. W. Taft, *Chem. Rev.* **1991**, *91*, 165–195.
- [27] F. Doro, J. N. H. Reek, P. W. N. M. van Leeuwen, *Organometallics* **2010**, *29*, 4440–4447.

Received: June 8, 2012
Published online: ■■■■, 0000

Supramolecular bidentate ligands: A new class of supramolecular hybrid bidentate phosphane–phosphoramidite ligands is presented (see scheme). The coordination behaviour of these ligands was studied under hydroformylation conditions, showing formation of a single active species, the $[\text{RhH}(\text{CO})_2(\text{phosphane-phosphoramidite})]$ complex, in which the phosphoramidite occupies the equatorial position and the phosphane occupies the apical position. In the asymmetric hydroformylation of styrene and *para*-substituted analogues an influence of electronically different zinc(II)-templates on the activity and selectivity of the reaction is observed.



Ligand Design

R. Bellini, J. N. H. Reek . . .* ■■■■–■■■■

Application of Supramolecular Bidentate Hybrid Ligands in Asymmetric Hydroformylation